Spectrally selective IR thermography to accurate temperature measurement on ultra-thin rPET films

by R. Gilblas*, A. Singer*, P.-Y. Linot**, A. Lieurey*, F. Schmidt*

* *Univ Toulouse, IMT Albi, INSA Toulouse, ISAE-SUPAERO, CNRS, ICA, Albi, France*
** *Sleever Technologies, Saint-Sulpice, France*

Abstract

Ultra-thin polymer films are widely used in industry in various domains like coating, packaging, surface functionalization or labelling. To produce or shape them, initial thermoplastic polymers are exposed to moderate temperature ranges (from room temperature to 250°C), to exploit their softening in various processes. The energy and performance optimizations of these processes faces a major challenge: In situ temperature measurement of thin films is highly challenging due to the semi-transparency appearing at small thicknesses, even in the IR spectral domain. This article presents the development of a thermography-based method, enabling accurate temperature measurement for rPET thin-films in the [20-150] °C range. This development relies on an advanced spectroscopic analysis of the IR transmission of the sample and on a rigorous metrology approach (calibration and validation bench test). The method demonstrates promising results on an in-lab test bench.

1. Introduction

Ultra-thin recycled polyethylene terephthalate (rPET) polymer films, with thicknesses ranging from 20 to 200 µm, are widely used in applications such as coating, packaging [1], surface functionalization [2], and labelling. Several industrial deposition processes operate at non-ambient temperatures, typically between 20 and 120 °C, making accurate temperature monitoring of these films essential. However, the thermo-optical properties of rPET may vary significantly due to differences in pellet origin, recycling technologies, virgin-to-recycled PET ratios in the formulation, and local thickness variations, which challenges conventional temperature measurement methods [3].

At such small thicknesses (from 20 to 200 µm), standard infrared thermography is strongly affected by semi-transparency over a broad spectral range (from 0.4 to 20 µm). The thermal radiation is emitted throughout the entire thickness of the film, which may exhibit a non-isothermal temperature distribution. Determining the temperature at a specific location within the material's thickness presents a significant challenge, necessitating the implementation of sophisticated inversion methodologies and multispectral detection techniques that fall beyond the purview of the present study. Secondly, radiation transmitted through the film may contaminate the measured signal, leading to significant temperature errors. These effects become negligible in the infrared only for thicknesses exceeding approximately 1 mm.

The existing literature exhibits limited exploration of thermographic techniques applied to thin polymer films. In reference [4], indium tin oxide (ITO) coatings were deposited onto (PET) substrates, where an infrared (IR) camera was employed to capture thermal images for defect detection and thermal metrology purposes. The inherent semi-transparency of PET did not pose a significant obstacle in this context. Meanwhile, study [5] focuses on monitoring acetone evaporation from polymer films, wherein the IR camera demonstrated sensitivity to the presence or absence of the liquid phase. However, this article doesn't mention any need absolute temperature quantification. Similarly, Greppmair et al. [6] proposed a methodology for characterizing the thermal properties of thin polymer films by analyzing their thermal response following radiative excitation at short wavelengths. The measurements were conducted at longer wavelengths, resulting in the mitigation of parasitic effects. Notably, absolute temperature measurements were not necessary, as relative temperature variations sufficed for the development of predictive models leading to thermal property identification.

This work presents the development of a spectrally selective thermographic method specifically designed for ultra-thin rPET films. The approach relies on the use of an interference filter targeting the strongest infrared absorption bands of rPET, which are associated with the molecular vibrational modes of the polymer. By restricting the measurement to these spectral regions, effective opacity is achieved even for very small thicknesses, thereby restoring the assumptions required for classical infrared thermography.

The study begins with a spectral characterization of rPET using FTIR spectroscopy, enabling the quantitative identification of absorption coefficients (in cm-1) through transmission and reflection measurements. At the selected absorption band, the transparency of rPET diminishes significantly, rendering it effectively opaque when its thickness exceeds 10 µm.

Subsequently, the µ-bolometer technology IR camera FLIR® A655SC, operating in the [7.5-13] µm spectral range, outfitted with the designated interference filter, undergoes calibration across the temperature range [30–150] °C by means of a standardized blackbody reference. The impact of spectral filtering on sensor performance (sensitivity, NEDT, and usable temperature range) is then assessed. Even though the dynamic range of the IR camera exhibits significant degradation, the implementation of an appropriate calibration model effectively minimizes interpolation artifacts, thereby ensuring high fidelity in the resulting data.

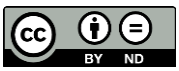

Finally, the proposed method is validated experimentally on an ultra-thin rPET film heated by an infrared emitter, with thermographic measurements compared to temperatures obtained from a contact sensor. The observed temperature deviation across the entire thermal range remains consistently below 10°C.

2. IR absorption coefficient characterization by spectroscopy

2.1. Methodology

The accuracy of temperature measurements via thermographic techniques on semi-transparent materials requires several critical conditions to be fulfilled. Firstly, it is imperative that the detected radiation originates from a superficial region where thermal gradients are negligible, i.e. within an isothermal domain. Under such conditions, the emitted radiation can be reliably correlated with the material's temperature, and the so-called emissivity of the material can be properly defined. Secondly, the sample must exhibit complete opacity to prevent the intrusion of parasitic radiation emanating from the rear, which could introduce an erroneous signal and distort the desired measurement. In the present study, where semi-transparency may pose a significant challenge due to the thinness of the samples, we undertake a meticulous characterization of their opacity via infrared (IR) spectrometry.

Kirchhoff's laws relate the radiative properties of semi-transparent materials at thermodynamical equilibrium:

$$\begin{cases} \tau_\lambda + \rho_\lambda + \alpha_\lambda = 1 \\ \alpha_\lambda = \varepsilon_\lambda \end{cases} \quad (1)$$

With: λ: wavelength (m); τ: transmission (Without Unity (W.U.)); ρ: reflectivity (W.U.); α: absorptivity (W.U.); ε: emissivity (W.U.)

The emissivity of a material, essential for an accurate measurement of temperature by thermography, can be identified indirectly through the reflectivity and transmission measurement by IR spectrometry.

The transmission depends on the thickness of the material and introduces the absorption coefficient k_{abs} (*in* m^{-1}), as an intrinsic optical parameter which defines the intensity decay per distance unit. For purely absorbing material (scattering is neglected) and neglecting self-emission of the sample, Beer-Lambert law relates this quantity to transmission:

$$\tau = (1 - \rho)\exp(-k_{abs}e) \quad (2)$$

With: e: sample thickness (m); k_{abs} *: absorption coefficient* (m^{-1})

The mean free path of photons (*MFP in m*) is defined as the inverse of the absorption coefficient:

$$MFP = \frac{1}{k_{abs}} \quad (3)$$

Opacity is achieved when the physical thickness *e* of the sample exceeds three times the MFP ($e > 3*MFP=3/k_{abs}$). The absorption coefficient serves as the critical metric for determining thermographically optimal wavelength bands, wherein accurate temperature quantification via surface emissivity is feasible—ensuring minimal parasitic transmission interference and maximizing detectable thermal emission.

The method used in this article consists in measuring the transmission by spectrometry for different thicknesses, and to identify the absorption coefficient through a linear regression of the logarithm of the transmission. This method faces two major challenges in the infrared domain:

- Capacity to prepare samples with controlled thicknesses. The method exhibits accurate results solely under conditions where the transmission coefficient deviates distinctly from the extreme values of 0 and 1, as these yield physically inconsistent absorption coefficients (i.e., infinite and null, respectively). Given the inherent noise levels in spectroscopic measurements (approximately 1% for the spectrometer employed in this study), we establish an acceptable transmission range of [1%–99%]. Outside this defined interval, reliable identification of the absorption coefficient becomes unfeasible.
- Interferences at film-scale. When assessing the transmission properties of low-thickness semi-transparent specimens, the global transmission originates both from the direct transmission, but also from the contribution of the ray that travels inside the sample due to multiple internal reflections within the sample (see. Fig. 1). Spectrometry measurements inherently yield only apparent values, necessitating a mathematical or optical model-based transformation to derive the intrinsic optical properties of the material.

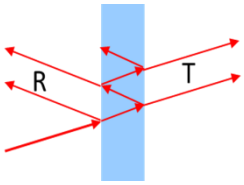

Figure 1. Illustration of apparent/intrinsic parameters relation

Howell [7] proposes a model relating apparent coefficients (T_λ *and* R_λ) to intrinsic ones (τ_λ *and* ρ_λ). One can note that, for thick samples, the transmission is null and the apparent reflectivity is equal to the intrinsic one ($R=\rho$).

$$\begin{cases} T_\lambda = \dfrac{(1-\rho_\lambda)^2\tau_\lambda}{1-(\rho_\lambda\tau_\lambda)^2} \\ R_\lambda = \rho_\lambda\left[1+\tau_\lambda^2\dfrac{(1-\rho_\lambda)^2\tau_\lambda^2}{1-(\rho_\lambda\tau_\lambda)^2}\right] \end{cases} \quad (4)$$

In this article, the transmission will be measured for several thicknesses of thin samples.

Due to the complexity of measuring reflectivity in samples of minimal thickness, an alternative approach will be employed wherein reflectivity measurements are conducted on a sample with a standardized thickness of 3 mm. It has been proven [3] that, for a 3mm thickness sample, rPET is completely opaque above 5µm wavelength ($R_\lambda=\rho_\lambda$). Given the assumption that intrinsic reflectivity exhibits thickness independence, indicating its surface-dependent nature, this parameter may be injected into Equ.4 to enable the computation of intrinsic transmission.

After the intrinsic parameters' retrieval, the methodology for determining the absorption coefficient involves calculating the natural logarithm of the intrinsic transmission across a range of sample thicknesses. Subsequently, a linear regression analysis is conducted on these logarithmic values. Should the coefficient of determination (R^2) exceed the threshold of 0.80, this indicates consistency to the Beer-Lambert law and validates the absorption coefficient value.

2.2. Sample preparation and spectroscopy equipment

Due to the prominence of absorption on the middle IR, it is necessary to elaborate very thin samples of rPET to have an exploitable transmission (i.e. between 1 and 99%). A series of samples were produced by thermocompression using a Specac® hydraulic press (as illustrated in Fig. 2). Specifically, a 50 wt% composition was synthesized by blending recycled PET pellets with virgin PET pellets in a weight ratio of (50:50).

To achieve quasi-amorphous structures in rPET, the selected processing temperature of 225°C must lie within the thermodynamic window defined by the crystallization onset temperature (175°C) and the melting point (245°C), as previously reported in the literature [8]. The temperature-pressure cycle used is shown in Fig. 2.

a) 

b) 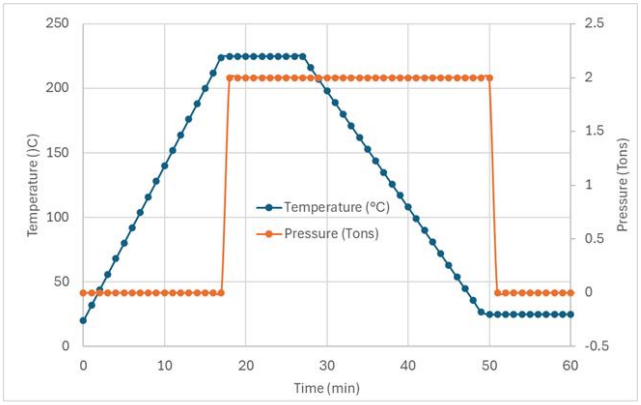

Figure 2. Sample preparation: a) Hot press picture; b) Temperature/pressure cycle

The thermal treatment protocol involves an initial ramp-heating phase wherein the system is elevated from ambient temperature to 225 °C over a duration of 17 min, followed by an isothermal hold at this elevated temperature while subjecting the sample to a constant load of 2 tons for 10 min. Subsequently, the temperature is decremented back to ambient conditions over 23 minutes, after which the applied pressure is relieved, and the treated sample is retrieved for further analysis.

Using this methodology, seven thin samples and one thick sample were prepared, and their thicknesses have been verified by a Fisher® Isoscope Eddy Current probe, enabling thickness measurements of dielectric materials from 10 µm to 0.5 mm. The thicknesses obtained are presented in table 1:

Table 1. *Thicknesses of the samples prepared*

Sample number	1	2	3	4	5	6	7	8
Thicknesses (µm)	14.7	23.7	40.4	58.2	84.6	111.3	167.8	3000

Ultra-thin rPET samples were prepared (14.7µm) to ensure high transmission levels, even in strong absorption spectral domains. The first 7 thicknesses will be used for the linear regression, which is enough to guarantee trustful results.

The samples are positioned in a spectrometer Bruker® Vertex 70 FTIR (Fourier Transform InfraRed) spectrometer, equipped with a DLaTGS detector, enabling measurements in the range [2.5-20] µm. This wide spectral band is justified by the will to find narrow absorption bands included in the spectral response ([2.5-5]µm and [7.5-13]µm) of IR cameras commonly used in polymer processing. A 1500 K Globar® SiC source is used as an infrared emitter. Two units are necessary for transmission and reflection measurements, described in Fig.3.

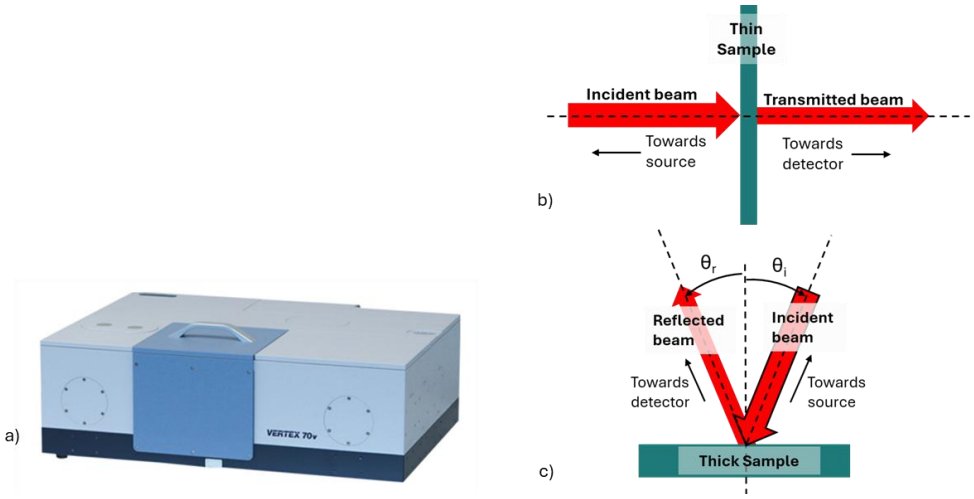

Figure 3. Equipment used for spectrometry characterization: a) Picture of the Bruker Vertex 70; b) Unidirectional unit for transmission measurement; c) Goniometer unit used for reflectivity measurement.

The transmission unit is performed with incident and transmission angles of 0°, whereas the reflection unit performs its measurement for $\theta_i = \theta_r = 13°$. We suppose in this article that this slight variation in incident angle is negligible, and that energy conservation equation (Equ.1) is still valid.

2.3. Characterization results

The first step of the characterization consists in converting apparent transmission to intrinsic one. Fig. 4 compares the apparent (T) to the intrinsic (τ) transmission spectrum of the thinnest sample (*e=14.7 µm*). Additionally, the figure quantifies the relative percentage discrepancy between the two-transmission metrics.

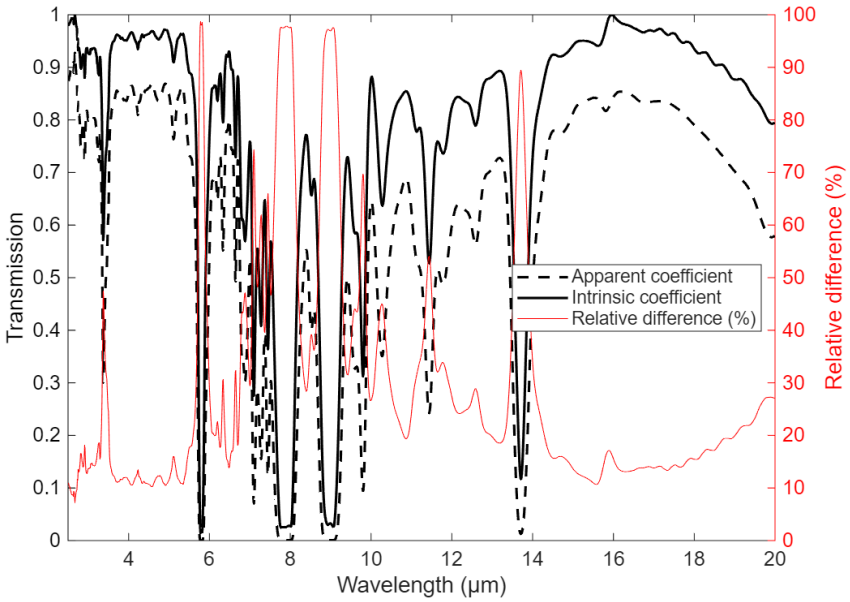

Figure 4. Transmission spectrum for the 14.7µm thin rPET sample: difference between apparent and intrinsic properties

The analysis of the transmissions on this figure clearly demonstrates that the intrinsic transmission is roughly 30% superior to the apparent one, with peak values reaching 95% in the absorption bands. This difference highlights the importance of considering intrinsic parameters in the absorption coefficient computation. Indeed, if transmission is underestimated, the absorption coefficient will be overestimated.

Fig.5 shows the intrinsic transmission spectrum of 4 selected samples, and the intrinsic reflectivity ρ (equal to R) of sample 8.

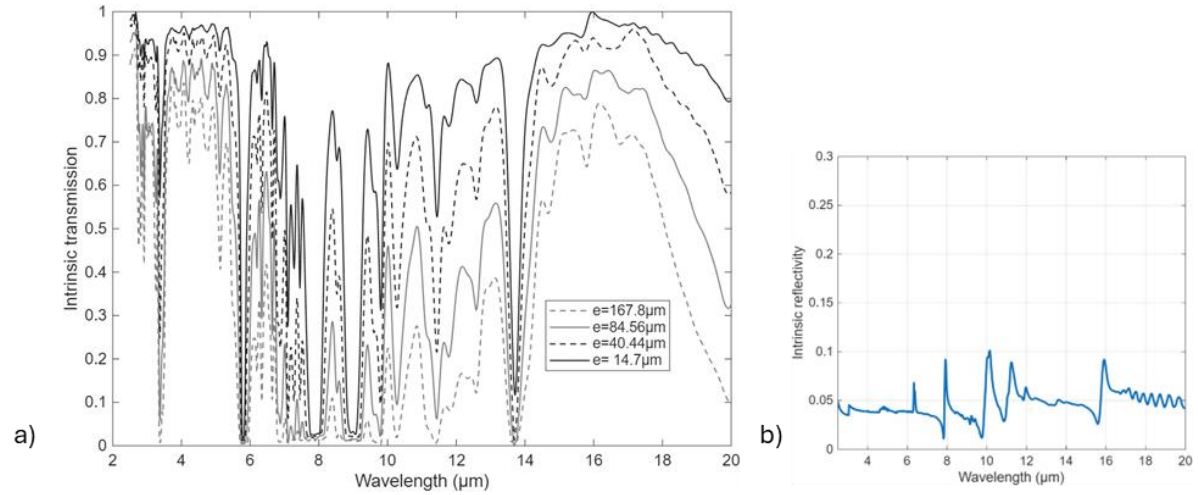

Figure 5. a) Intrinsic transmission spectrum for samples 1, 3, 5, and 7; b) Intrinsic reflectivity for sample 8.

As predicted by Beer-Lambert's law, the transmission decreases with thickness. The transmission values are generally between 0 to 1, which justifies the selected range of thicknesses discussed earlier in the article. However, some spectral bands (at 8, 9 and 13.7 µm) are still strongly absorbing (i.e. transmission inferior to 5%), even for the thinnest thickness. The absolute value of the absorption coefficient will not be possible for these spectral bands. Alternatively, the reflectivity spectrum displays low values (around 4%) with some peaks reaching 10%. This result is classical for reflectivity of polymers in this spectral range [3].

The absorption coefficient obtained after linear regression of the intrinsic transmission logarithm versus thickness is displayed in Fig. 6, with an example of linear regression performed at the arbitrary wavelength of 10.4 µm. The spectral bands of strong absorption, denoted by a determination coefficient $R^2<0.8$, are highlighted. In these areas, the absolute identification of the absorption coefficient has not been possible due to too low transmission.

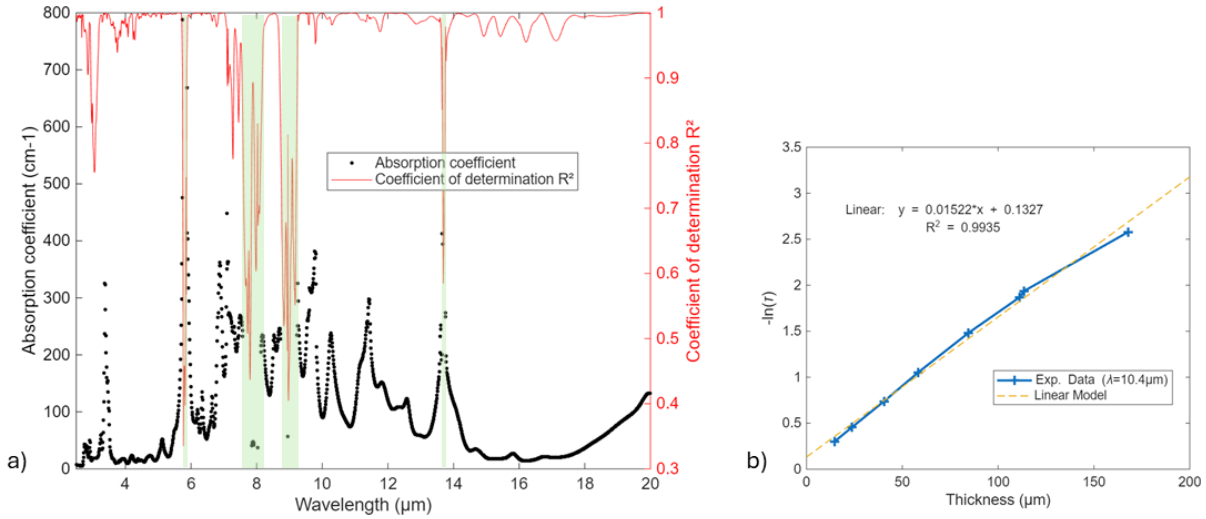

Figure 6. a) Absorption coefficient and coefficient of determination R^2 of the linear regression; b) Linear fit of the logarithm of transmission versus thickness at 10.4 µm

The strongest absorption bands are located between 5 and 15 µm, with absorption coefficient values superior to 250 cm^{-1}. With such absorption coefficient, the opacity is reached for a thickness of 120 µm. The requirements of the study mention 50 µm films, which requires an absorption coefficient above 600 cm^{-1}. These values can only be obtained in the strongest absorption bands, located at 8 and 9 µm, even though absolute values of absorption coefficient and/or opacity limit are not possible.

3. Development of a thermography-based method adapted to rPET thin films

This section treats the development of the thermography method development to perform temperature measurement on ultra-thin rPET samples.

3.1. Camera and interference filter selection and accuracy prediction

Referring to Fig.6, a), the strongest absorption bands are in the range [5-15] µm. It is therefore unnecessary to use a camera which spectral bandwidth is comprised in [2.5-5] µm, like InSb detectors for instance. It seems more appropriate to use a camera operating at higher wavelength, as [7.5-14] µm for the microbolometer technology detectors. The selected camera, the FLIR® A655SC, is therefore a microbolometer-based detector laboratory blackbody were placed. Its main characteristics are given in Tab. 2.

Table 2. *Characteristics of the FLIR A655SC camera*

Spectral bandwidth (µm)	Resolution (pixels²)	Pixel Pitch (µm)	Max. frequency in full frame (Hz)	Number of bits	Focal length (mm)
[7.5-14]	640*480	17	50	16	24.6

The selection of the filters used to select the absorption bands resides in a compromise: it must be narrow enough to reject the transparency bands around the absorption band and it has to be large enough to induce sufficient signal on the camera. Note that bichromatic thermography could be developed for at 8 and 9 µm but wouldn't present any interest as emissivity is known, high (0.92) and stable within the absorption bands. Monochromatic thermography is then sufficient for the requirements of this study. The characteristics of the chosen filter, manufactured by Northumbria Coatings® company, are given in Tab.3.

Table 3. *Characteristics of the chosen filter*

Central wavelength (µm)	FWHM (nm)	Transmission at central wavelength (%)
9.1	300	87

This filter is inserted between the lens and the detector to narrow down the spectral response.

Referring to Equ.1, and having available the transmission and reflection of the polymer, it is possible to calculate the emissivity of rPET for the wavelength selected by the interference filter. This value is equal to ε=0.92 and is valid for the whole thickness and thermal range. This parameter will serve as a configurable setting for the thermography temperature retrieval processes.

3.2. Calibration of the system

As the spectral response were modified by the addition of a filter in the optical path, it is necessary to re-calibrate the system. Hence, a laboratory blackbody was placed in front of the camera and its temperature is controlled between in the range [40-160]°C with a step of 20°C. Once thermal stabilisation is achieved, the acquisition of 60 images at 1Hz frequency is performed. The spatial average of the pixels inside the blackbody aperture is displayed in Fig.7. Note that the background digital levels were subtracted from the raw digital levels.

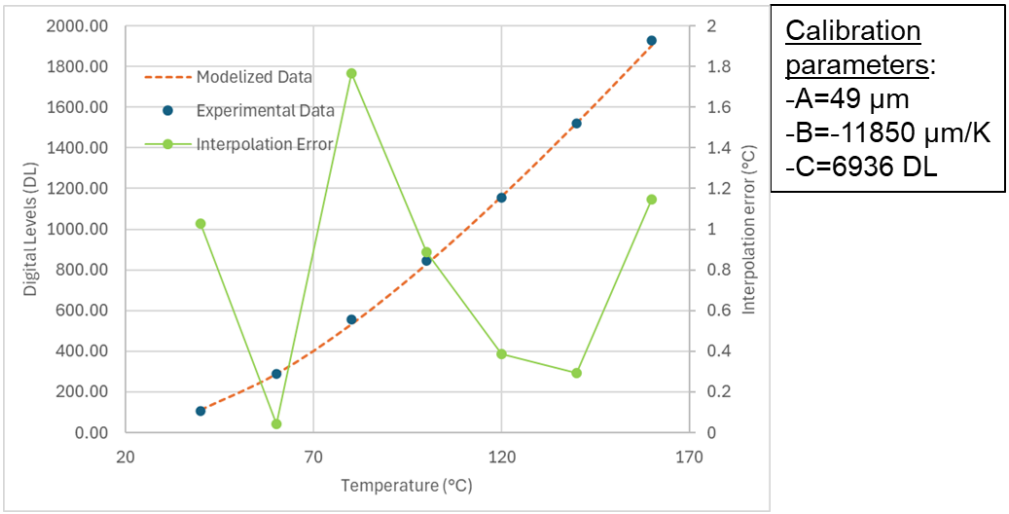

Figure 7. Calibration curve, Sakuma Hattori model superposition and interpolation error

Among all the variety of interpolation models available in the literature [9], the choice was made in this study to use the Sakuma-Hattori model in its Planck version. Indeed, Wien's version (λT<3000 µm.K) is not adapted to our thermal and spectral range. This model is recalled hereafter:

$$S(T) = \frac{C}{\exp\left(\frac{C_2}{AT+B}\right)-1} \quad (5)$$

With: *S(T): Digital levels recorded by the camera [DL]; C_2=14388 µm.K: Second Planck's constant; A [µm], B [µm.K], C [DL] : Calibration parameters.*

The parameters A, B and C were determined by numerical resolution using Matlab® and are presented in Fig. 7. The resulting absolute error between the temperatures retrieved by the model and the experimental points is also computed and displayed on the figure. This interpolation error does not exceed 2°C, which satisfies the requirements of this study.

The assessment of the interference filter's integration within the optical pathway was further examined by evaluating its impact on key metrological performance metrics, specifically the digital levels range (DLR), sensitivity (K), and noise-equivalent differential temperature (NEDT). These parameters can be estimated thanks to the calibration data. The digital level range is the difference between the digital levels obtained at the maximal temperature (T_N=160 C°) and the ones at the minimum temperature (T_1=40 °C). Sensitivity is approximated by the coefficient of the linear trend linking two consecutive points. The noise of the camera is computed as the spatial average of the temporal standard deviation of each pixel over a set of stable images (obscurity images). Finally, NEDT (Noise Equivalent Differential Temperature), is calculated dividing this noise by the minimum sensitivity over the thermal range:

$$\begin{cases} DLR = DL(T_N) - DL(T_1) \\ K_i = \frac{d(S(T))}{dT} \approx \frac{\Delta S(T)}{\Delta T} = \frac{S(T_{i+1})-S(T_i)}{T_{i+1}-T_i} \\ NEDT = \frac{\sigma_{DL}}{\min(K_i)} \end{cases} \quad (6)$$

With: K: Sensitivity of the measurement [DL/°C]; NEDT (Noise Equivalent Temperature Detected) [°C]; σ_{DL} : Camera noise standard deviation [DL]

The comparison of the metrological parameters with and without filter are gathered in Tab.4.

Table 4. *Effect of the interference filter on the metrological parameters of the camera*

	DLR *[DL]*	σ_{DL}*[DL]*	Min(K) *[DL.°C^{-1}]*	NEDT *[°C]*
Configuration without filter	41775	12	254	0.047
Configuration with filter	2650		16	0.750

The introduction of an interference filter in the optical path clearly decreases the DLR by almost 94%. This phenomenon is due to the reduction of the spectral bandwidth of the detector, evolving from 6.5 to 0.3 µm. The temporal noise is equal to 12 DL and remains constant with or without filter. Sensitivity is also greatly lowered to 16 DL.°C^{-1}, and, consequently, the NEDT increases. It reaches the value of 750mK, which is the minimum temperature difference that can be detected with this method. It is still compatible with the specifications of our study.

Once the calibration law and parameters fixed, with the metrological parameters' limitations known, the inverse law enabling to convert digital levels to temperature is given in Equ. 6, which includes emissivity (equal to 0.92 for rPET as stated before):

$$T = \frac{C_2}{\exp\left(\frac{C\,\varepsilon}{S}+1\right)} - \frac{B}{A} \quad (7)$$

3.3. Test of the method on a reference bench

The test of the method will be performed on a 50µm thin film rPET. Two types of validation are performed: the opacity verification and the temperature trueness estimation. The first experiment, at room temperature, consists in detecting the radiation emitted from an IR source and to insert a thin rPET film between the emitter and the detector. If the opacity is reached, no signal should be detected. The second experiment consists of comparing the temperature retrieved by this method with the one provided by a Pt probe. Pictures of the two experiments are gathered in Fig.8.

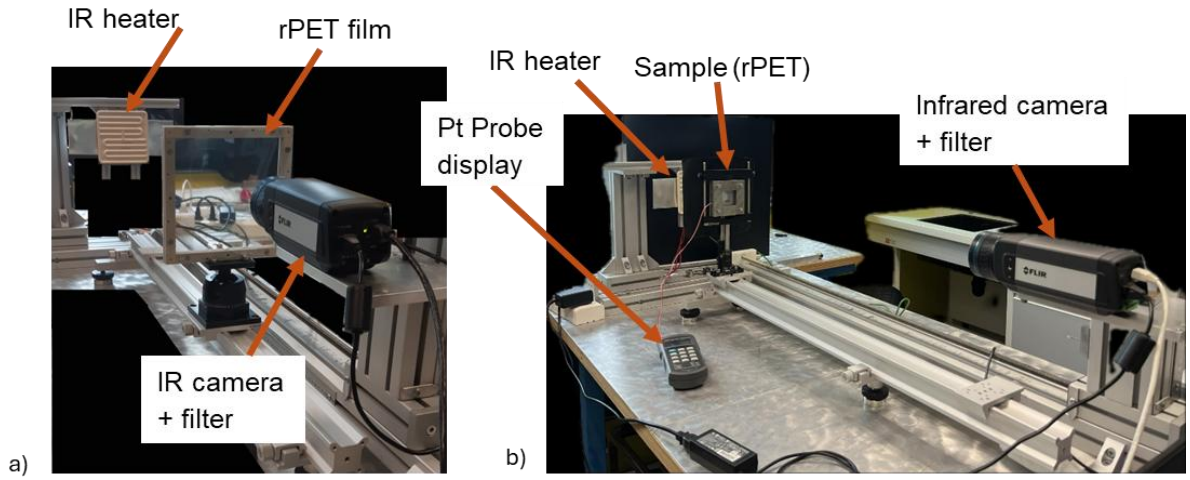

Figure 8. Picture of the test bench for a) Opacity verification; b) Temperature measurement

3.3.1. Opacity verification

The IR camera, alternately configured with and without an interference filter, was directed toward an Elstein® IR emitter maintained at a stabilized low temperature of 246°C and positioned at 1.5m. The flux received by the film is therefore very low and its temperature remains close to room temperature, which limits self-emission. A 10*10cm² and 50µm in thickness rPET film is placed 10cm from the IR camera and is used as an optical window (see Fig.8.a). IR images are recorded in the different configurations to analyse the effect of both filter and rPET on the opacity. Fig.9 displays an image assembly of the different observations.

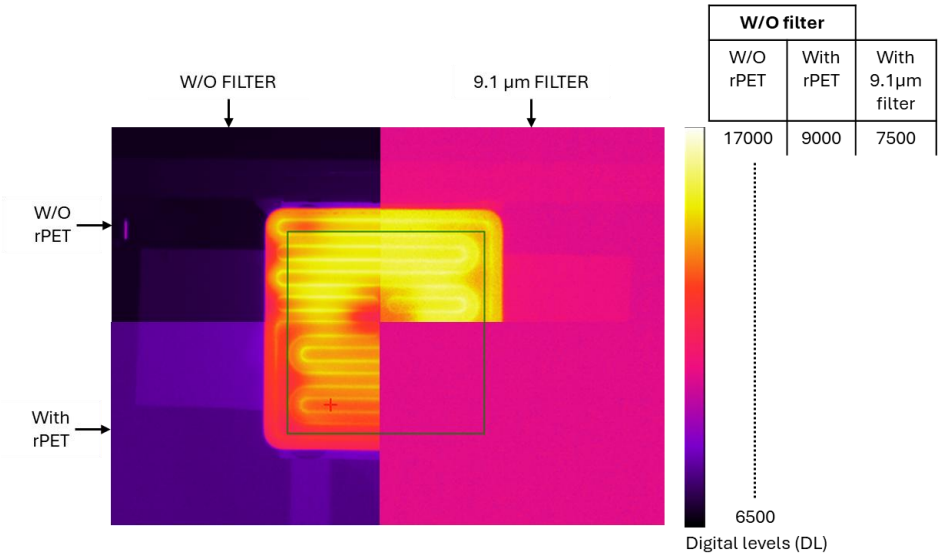

Figure 9. Image assembly of IR images of the infrared emitter: Top/left: w/o filter, w/o rPET; Top/right: with filter, w/o rPET; Bottom/left: w/o filter, with rPET; Bottom right: with filter, with rPET.

The direct observation of the emitter (Top, left) without the interference filter (whole spectral band of the camera) provides a clear image of the emitter, with digital levels ranging from 6500 to 17000 DL. Adding the rPET between the emitter and the camera (bottom, left) still displays the emitter image, even though it has been drastically attenuated (maximum DL value of 9000). Without any filter in its spectral response, opacity conditions are clearly not achieved.

When adding the 9.1µm interference filter (Top, Right), the image is still clear, even though the range has dropped down to [6500-7500] DL. This is the effect of the interference filter which narrows the spectral response of the camera. Finally, adding the rPET film between the camera and the emitter (Bottom, Right), this latter completely disappears and shows an average value of 6880 DL, which is identical to the background value, when the lens is completely covered. This result confirms that our camera equipped with an interference filter centred at 9.1µm and with a FWHM of 300nm operates in the opacity spectral domain of rPET. There is therefore no risk of parasitic radiation coming from behind the sample and degrading the signal.

3.3.2. Temperature measurements

For this test, a 4cm² square sample, 50µm in thickness, is cut and inserted in an isolating frame to guarantee flatness of the sample and to prevent heat leakage (see Fig.8, b). This frame is placed near the emitter (10cm) to maximize the rPET film heating. A circular diaphragm is inserted between the emitter and the sample to localise the heat flux on the rPET film. A Pt probe is bonded on the emitter side of the sample to provide a comparison temperature. Due to the very small thickness of the sample, one can consider that the thermal gradient across the thickness can be neglected. Indeed, the computation of Biot Number ($Bi = h\ e\ /\ \lambda$), with h≈10 $W.m^{-2}.K^{-1}$ (heat transfer coefficient), e=50µm (thickness) and λ≈0.15 $W.m^{-1}.K^{-1}$ (thermal conductivity of rPET) provides a value of $3.33.10^{-3}$, which is largely inferior to unity. This result confirms that thickness thermal gradient is null.

Three emitter temperatures are tested (307, 375 and 416°C) and IR images are recorded once the stationary regime is reached. For each configuration, 60 images are recorded at 1 Hz frequency, and an average image is computed. The average IR image obtained with an emitter temperature of 416°C is presented Fig.10.

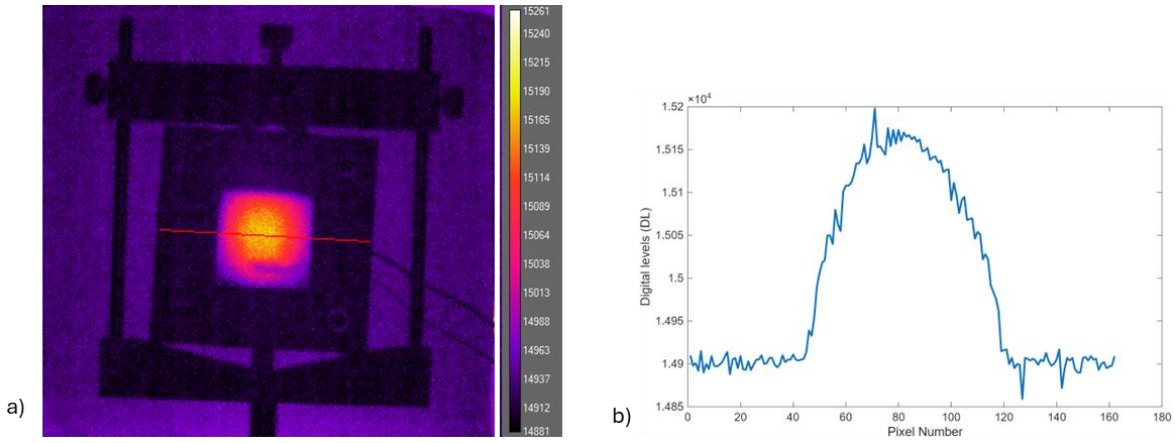

Figure 10. a) Infrared image of the 50µm thin rPET film heated by the IR source stabilized at 416°C; b) Horizontal temperature profile across the sample.

Pt probe temperatures are also recorded for each emitter temperature. They are displayed in Tab. 5, along with the results of the temperature obtained by thermography. This latter is computed by exploiting the spatial average of a small ROI (Region Of Interest) located near the probe, and by applying Equ.7.

Table 5. *Results of the temperature measurement on the 50µm thin film*

Emitter temperature (°C)	Camera temperature (°C)	Pt probe Temperature (°C)
307	35	33
375	47	41
416	54	46

Firstly, both methods exhibit the low temperature of the rPET sample. This is mainly due to the low radiation send by the emitter, narrowed by the diaphragm and intercepted by the sample. However, both methods achieve to record an increasing temperature while increasing the regulation temperature of the emitter. Both methods are therefore sensitive to temperature variations, even for relatively low increments.

Still, a deviation exists between the two sensors, which increases with temperature. It reaches 8°C for an emitter temperature of 416°C. It is difficult to determine which measurement technique is responsible for the observed discrepancy. On one hand, the major drawback of the thermography method is the low digital level range induced by the interference filter. In those conditions, signal to noise ratio is not optimal. On the other hand, measurement with a sticked Pt probe on thin films polymers raises several interrogations: the thermal contact between the probe and the films might be incorrect and the absorption of the probe regarded the emitter radiation might be different from the rPET one, resulting in an excessive local temperature.

4. Conclusion

This study addresses the challenge of non-contact temperature measurement of ultra-thin rPET films via IR thermography. The proposed methodology is based on the advanced characterisation of the absorption coefficient of the material, which is an intrinsic parameter enabling the precise identification of opacity and transparency bands. Samples preparation has been a challenging task, as the thickness compatible with a transmission comprised in [1-99] % range is very low. The thinnest sample of 14.7µm has been successfully elaborated via hot-press moulding.

Once the absorption coefficient determined, the identification of the thermography-compatible spectral bands have been performed. Wavelengths located around 9µm have been selected, as they promise a deep opacity, obtained for thicknesses at least superior to 120µm. Experimental verification confirmed this prediction, and revealed that opacity is reached for a 50µm thickness.

To ensure measurement accuracy, the IR camera system equipped with its interference filter was calibrated using a blackbody reference source and employing the Sakuma-Hattori (Planckian) model for digital levels interpolation. The calibration exhibited substantial fidelity, with interpolation errors remaining below 2°C across the [40–160]°C operational range.

The methodological validation involved radiative heating of the rPET films via an IR emitter, with temperature measurements obtained via thermography and compared against a Pt probe). While the results demonstrated close agreement, minor deviations were observed, suggesting potential avenues for refinement. Nonetheless, these preliminary findings underscore the feasibility of thermographic monitoring for thin, semi-transparent polymeric structures, offering promising applications in thermal diagnostics and process control.

Future research directions may focus on metrological improvements. In particular, the availability of a reliable reference temperature sensor for thin rPET films would enable a rigorous assessment of measurement trueness. Another way would be to perform the same methodology on other materials and other temperatures. Additionally, optical characterization at sub-micron thicknesses could enable the absolute quantification of absorption coefficients within deep absorption bands, further refining the methodology's precision.

References

[1] M. A. Hubbe *et al.*, « Nanocellulose in Thin Films, Coatings, and Plies for Packaging Applications: A Review », *BioRes*, vol. 12, nº 1, p. 2143-2233, févr. 2017, doi: 10.15376/biores.12.1.2143-2233.

[2] A. Khlyustova, Y. Cheng, et R. Yang, « Vapor-deposited functional polymer thin films in biological applications », *J. Mater. Chem. B*, vol. 8, nº 31, p. 6588-6609, 2020, doi: 10.1039/D0TB00681E.

[3] A.-D. Le, R. Gilblas, V. Lucin, Y. L. Maoult, et F. Schmidt, « Infrared heating modeling of recycled PET preforms in injection stretch blow molding process », *International Journal of Thermal Sciences*, vol. 181, p. 107762, nov. 2022, doi: 10.1016/j.ijthermalsci.2022.107762.

[4] K. Remes, K. Leppänen, et T. Fabritius, « Thermography based online characterization of conductive thin films in large-scale electronics fabrication », *Opt. Express*, vol. 26, nº 2, p. 1219, janv. 2018, doi: 10.1364/OE.26.001219.

[5] A. R. Greenberg, S. S. Shojaie, W. B. Krantz, et S. B. Tantekin-Ersolmaz, « Use of infrared thermography for temperature measurement during evaporative casting of thin polymeric films », *Journal of Membrane Science*, vol. 107, nº 3, p. 249-261, nov. 1995, doi: 10.1016/0376-7388(95)00123-2.

[6] A. Greppmair, N. Galfe, K. Amend, M. Stutzmann, et M. S. Brandt, « Thermal characterization of thin films via dynamic infrared thermography », *Review of Scientific Instruments*, vol. 90, nº 4, p. 044903, avr. 2019, doi: 10.1063/1.5067400.

[7] J. R. Howell, M. P. Mengüç, K. Daun, et R. Siegel, *Thermal Radiation Heat Transfer*, 7e éd. Seventh edition. | Boca Raton : CRC Press, 2021. | Revised edition of: Thermal radiation heat transfer / John R. Howell, M. Pinar Mengüç, Robert Siegel. Sixth edition. 2015.: CRC Press, 2020. doi: 10.1201/9780429327308.

[8] L. Viora *et al.*, « A Comparative Study on Crystallisation for Virgin and Recycled Polyethylene Terephthalate (PET): Multiscale Effects on Physico-Mechanical Properties », *Polymers*, vol. 15, nº 23, p. 4613, déc. 2023, doi: 10.3390/polym15234613.

[9] P. Saunders, « Calibration and use of low-temperature direct-reading radiation thermometers », *Meas. Sci. Technol.*, vol. 20, nº 2, p. 025104, févr. 2009, doi: 10.1088/0957-0233/20/2/025104.